

Physics-penalised Regularisation for Learning Dynamics Models with Contact

Gabriella Pizzuto

GPIZZUTO@ED.AC.UK

Michael Mistry

MMISTRY@ED.AC.UK

School of Informatics,

Institute of Perception, Action and Behaviour;

University of Edinburgh,

United Kingdom

Abstract

Robotic systems, such as legged robots and manipulators, often handle states which involve ground impact or interaction with objects present in their surroundings; both of which are physically driven by contact. Dynamics model learning tends to focus on continuous motion, yielding poor results when deployed on real systems exposed to non-smooth frictional discontinuities. Inspired by a recent promising direction in machine learning, in this work we present a novel method for learning dynamics models undergoing contact by augmenting data-driven deep models with physics-penalised regularisation. Precisely, this paper conceptually formalises a novel framework for using an impenetrability component in the physics-based loss function directly within the learning objective of neural networks. Our results demonstrate that our method shows superior performance to using normal deep models for learning non-smooth dynamics models of robotic manipulators, strengthening their potential for deployment in contact-rich environments.

Keywords: Dynamics Model Learning, Physics-guided Learning

1. Introduction

Robust manipulation is a fundamental prerequisite of robotic platforms for efficient interaction outside carefully designed environments. For example, the utilisation of robots in industrial settings such as nuclear decommissioning ([Marturi et al. \(2017\)](#)) and manufacturing plants ([Garcia et al. \(2006\)](#)) relies heavily on contact-rich manipulation, where robots have to manoeuvre in partially unknown environments utilising noisy and incomplete sensory information. As a result, manipulators would greatly benefit from an explicit understanding of how to deal with unpredicted contact.

During physical interaction, contact is a complex phenomenon following near impulsive forces for a small duration of time, possibly leading to local deformations ([Parmar et al. \(2020\)](#)). For instance, when a robot manipulates an object, it can pick up or push the object, in addition to potential object slippage ([Fazeli et al. \(2020\)](#)). Consequently the interaction would be attributed to different modes such as sticking or sliding. Stemming from this nature of contact, dynamics governing the interaction between contacting bodies are inherently non-smooth and governed by non-convex constraints ([Halm and Posa \(2019\)](#)). Hence robotic controllers exhibit shortcomings as most rely on smooth dynamics models. Moreover, these controllers are desired to have adequate compliance at contact as this is also an essential requirement for safe interaction with humans.

Model-based approaches ([Nguyen-Tuong and Peters \(2011\)](#), [Siciliano and Khatib \(2016\)](#)) are very appealing for compliant control. As these methods allow for significantly lower feedback gains whilst also guaranteeing high tracking performance, they have led to compelling results in the robotics field, ranging from bi-manual manipulation ([Azad et al. \(2016\)](#)) to whole-body humanoid control ([Sentis \(2010\)](#)). However, on one side, parametric approaches suffer from being cost-ineffective emanating from sample-complexity and lacking the inclusion of explicitly accounting for contact. On the other hand, data-driven methods exhibit shortcomings when modelling discontinuities and non-uniqueness in frictional impacts ([Parmar et al. \(2020\)](#)). In our work, we are especially interested in constraint-based robotic manipulation tasks where the dynamics are influenced by frictional interactions, still an open problem in dynamics model learning.

A potential solution is to leverage prior knowledge related to discontinuous dynamics directly in the learning process. In this aspect, the application of machine learning models for this scientific domain has yet to fulfill its potential with limited data and achieving robustness to out-of-distribution data, simultaneously producing physically consistent results ([Willard et al. \(2020\)](#)). Moreover, neural networks tend to suffer from inductive bias towards smooth motion and might violate the conservation principles governing physical laws. Given that the dynamics of a system follow some empirical rules or domain expertise, regularisation can encompass prior information by constraining the space of possible solutions ([Raissi et al. \(2017\)](#)). Encoding structured information in this manner enables the learning algorithm to gravitate towards physically plausible solutions and generalise with less data. In our case, for example, if we take a robot arm manipulating an object or interacting with the environment, it should be able to handle point contact or simultaneous contacts (for multiple bodies). In these cases, the system exhibits physical phenomena such that for instance, there should not be interpenetration between the bodies and normal forces can only act perpendicular to each other ([Lynch and Park \(2017\)](#)). Alas, this prior knowledge is omitted when using pure data-driven dynamics model learning. We hypothesise that if incorporated as a regulation mechanism can not only guide the learning process to converge to more physically plausible solutions, but will also make the robotic system safer for human robot interaction as it would penalise large forces accompanied with penetration.

Contributions. The main contribution of this paper is a novel formulation of the non-smooth dynamics learning problem that effectively combines the power of neural networks with prior knowledge, in the form of physics-based regularisation introduced directly in the end-to-end model. We achieve this by introducing a loss function that penalises interpenetration and ensures that the acceleration produced is perpendicular to the contact forces. The proposed method is evaluated on a learned non-smooth dynamics model in a non-prehensile manipulation task using a simulated Franka Emika Panda robotic manipulator. By doing so, we show that our learning approach with the proposed regularisation not only achieves better accuracy and is more interpretable, but successfully produces better predictions for non-smooth dynamics modelling, achieving better performance than a purely data-driven non-parametric model and generalises better across different slopes.

2. Related Work

Whilst there exists a large body of research focusing on direct and indirect dynamics model learning in manipulation ([Chua et al. \(2018\)](#), [Deisenroth et al. \(2011\)](#), [Lutter et al. \(2019\)](#), [Hitzler et al. \(2019\)](#)), in practice, the complexity of contact dynamics makes this a challenging endeavour as a result of partial observability, multi-modality, and stochasticity. Nonetheless, some do augment

their methods to take into account contact behaviour as for example [Calandra et al. \(2015\)](#) did focus on leveraging the continuity of the state-update equations in the contact forces and learning the mapping from current state and sensed contact forces to next state.

Recent works have also demonstrated that although neural networks, have excelled at learning physical phenomena, constraining the system when contacts are introduced remains a non-trivial problem for these universal function approximators ([Kloss et al. \(2017\)](#)). In their work, the authors highlighted the advantage of using an analytical model, i.e. predicting physically plausible solutions. Our method builds on their hypothesis, that encompassing prior knowledge from well-established physics-based models can lower the amount of training data and provides improved generalisation outside the training domain. There have been increased efforts in modelling discontinuities, where the focus has pivoted around learning parameterisations of inter-body signed distance and contact-frame Jacobians ([Pfrommer et al. \(2020\)](#)) or utilising residual physics for point contact learners ([Fazeli et al. \(2017\)](#)). Although these approaches result in rich descriptions of frictional contact, they either assume prior knowledge of what contacts are active or learn where and when discontinuous and non-smooth behaviours including impact and stick-slip transitions occur. However, it has not been demonstrated how these would perform in the presence of high-dimensional observational spaces as is the case for a manipulator with multiple degrees-of-freedom.

There has also been work related to data-augmented residual models ([Ajay et al. \(2018\)](#), [Jiang and Liu \(2018\)](#)) as it can be more efficient to learn the residual errors generated by the analytical models rather than an end-to-end model. For example, [Ajay et al. \(2018\)](#) leveraged neural models to correct the output of their model when approximating pushing outcomes. As with any other data-driven method, the predicted output could be physically impossible. Our approach addresses this problem through a physics-penalised regularisation method which guides the learning objective.

As recently the research community has started to focus on integrating scientific knowledge and data in a synergistic manner, one such way to achieve this is through constrained optimisation. This is another novel approach that aims to respect laws of physics during data-driven model learning by minimising violations of physical laws. Its motivation pivots around ensuring better model generalisation by anchoring algorithms with scientific knowledge, producing scientifically interpretable models and reducing the search space of the learning algorithm to physically consistent models for lower computational complexity ([Karpatne et al. \(2017\)](#), [Elhamod et al. \(2020\)](#)). The field of robotics would also gain from this paradigm, as it can build on years of physics and domain knowledge. For instance, [Asenov et al. \(2020\)](#) showed that using an additional loss in their variational recurrent neural network encourages encoding of physically meaningful parameters in their dynamics model.

[Pfrommer et al. \(2020\)](#) also proposed a structured approach for contact dynamics capable of circumventing numerical challenges emerging from discontinuities and is potentially the closest to our approach. As opposed to this model, our work adopts a physics-based loss directly in the end-to-end learning process, which is a non-trivial challenge as mentioned by [Kloss et al. \(2017\)](#). Our hypothesis is that modifying dynamics model learning in this manner when in the presence of contacts can greatly benefit from using penalty-based regularisation methods. These that directly encompass physics priors such as impenetrability in an attempt to overcome the discontinuous nature of frictional contact.

3. Background

Model-based control relies on forward or inverse dynamics models. Using Newton's second law of motion we can empirically formulate the equations governing the dynamics of a rigid body in free motion. For an open-chain robot, this is given by the following second-order differential equation:

$$\tau = \mathbf{M}(\mathbf{q})\ddot{\mathbf{q}} + \mathbf{h}(\mathbf{q}, \dot{\mathbf{q}}) \quad (1)$$

Equation 1 formulates the robot's inverse dynamics problem which determines the joint forces and torques required to fulfill the robot's desired joint accelerations for a given state. $\mathbf{q} \in \mathbb{R}^n$ represents the vector of joint variables for n degrees of freedom, $\tau \in \mathbb{R}^n$ is the vector of joint forces and torques, $\mathbf{M}(\mathbf{q}) \in \mathbb{R}^{n \times n}$ represents the symmetric positive-definite inertia matrix, $\mathbf{h}(\mathbf{q}, \dot{\mathbf{q}}) \in \mathbb{R}^n$ are forces stemming from the centripetal, Coriolis, gravitational and friction effects.

The forward dynamics problem distinguishes itself from the inverse as it computes the robot's joint acceleration $\ddot{\mathbf{q}}$ given the current state $(\mathbf{q}, \dot{\mathbf{q}})$ and joint forces and torques τ of the system.

$$\ddot{\mathbf{q}} = \mathbf{M}^{-1}(\mathbf{q})(\tau - \mathbf{h}(\mathbf{q}, \dot{\mathbf{q}})) \quad (2)$$

Given this formulation, we can now look into how the robot dynamics would change in constrained motion, for example where applied forces on the environment or on objects arise due to contact interactions. In this case, the robot is subjected to the following Pfaffian constraints ([Lynch and Park \(2017\)](#)):

$$\mathbf{J}_c(\mathbf{q})\dot{\mathbf{q}} = 0 \quad (3)$$

$\mathbf{J}_c(\mathbf{q}) \in \mathbb{R}^{k \times n}$ is the Jacobian matrix mapping the joint velocities to the Cartesian velocities at the external contact points, mathematically relating the contact point c , with k linearly independent constraints. These stem from closed loop constraints. Moreover, the time derivative of Equation 3, i.e. $\dot{\mathbf{J}}_c(\mathbf{q})\dot{\mathbf{q}} + \mathbf{J}_c(\mathbf{q})\ddot{\mathbf{q}}$ would also be equal to zero.

At the contact point, the generalised forces applied by the robot $\tau_c^T \dot{\mathbf{q}} = 0$. τ_c has to satisfy the criteria of being a linear combination of the columns of $\mathbf{J}_c^T(\mathbf{q})$, where $\tau_c = \mathbf{J}_c^T(\mathbf{q})\boldsymbol{\lambda}_c \forall \boldsymbol{\lambda}_c \in \mathbb{R}^k$. $\boldsymbol{\lambda}_c \in \mathbb{R}^{n_c}$ is the vector of generalised contact forces at the contact points n_c . These generalised forces should only work when $\dot{\mathbf{q}}$ does not violate the constraints in Equation 3, leading to:

$$(\mathbf{J}_c^T(\mathbf{q})\boldsymbol{\lambda}_c)^T \dot{\mathbf{q}} = \boldsymbol{\lambda}_c^T \mathbf{J}_c(\mathbf{q})\dot{\mathbf{q}} = 0 \forall \boldsymbol{\lambda}_c \in \mathbb{R}^k \quad (4)$$

When the constraint forces τ_c are added to the dynamics modelling equation (Equation 1), given that $\mathbf{M}(\mathbf{q})$ and $\mathbf{h}(\mathbf{q})$ are full rank, its constrained formulation becomes:

$$\tau = \mathbf{M}(\mathbf{q})\ddot{\mathbf{q}} + \mathbf{h}(\mathbf{q}, \dot{\mathbf{q}}) + \mathbf{J}_c^T(\mathbf{q})\boldsymbol{\lambda}_c \quad (5)$$

In this work, we will focus on a single contact point; however, it is worth mentioning that this model generalises to an arbitrary number of contact points.

From Equation 5, τ follows the laws of frictional contact where it will undergo non-smooth transitions and endure actuation limits from these interactions. The generalised joint forces τ are projected away from the constraints, simultaneously conserving the generalised forces working on the robot.

When two bodies are in contact, i.e. $\mathbf{d} = 0$, with \mathbf{d} being the distance from the surface to a potential contact point, the system is constrained within its three degrees of freedom ($p \in \{x, y, z\}$). In such a case, $\dot{\mathbf{d}} = \mathbf{J}_c \dot{\mathbf{q}}$ and $\ddot{\mathbf{d}} = \mathbf{J}_c \ddot{\mathbf{q}} + \dot{\mathbf{J}}_c \dot{\mathbf{q}}$. \mathbf{J}_c and $\dot{\mathbf{J}}_c$ hold information about the separation direction in joint space related to the unit surface normal vector, or contact normal \mathbf{u} , and the relative curvature of the bodies in contact respectively. When the bodies are in contact, \mathbf{u} is perpendicular to the contact tangent plane. As a result, the overall system will be subjected to the following constraint (Equation 6) and its second time derivative (Equation 7):

$$\mathbf{u}^T \dot{\mathbf{d}} \geq 0; \quad \mathbf{u}^T \mathbf{J}_c \dot{\mathbf{q}} \geq 0 \quad (6)$$

$$\mathbf{u}^T \ddot{\mathbf{d}} \geq 0; \quad \mathbf{u}^T (\mathbf{J}_c \ddot{\mathbf{q}} + \dot{\mathbf{J}}_c \dot{\mathbf{q}}) \geq 0 \quad (7)$$

Worth mentioning is the fact that the constraint given by Equation 6 and Equation 7 translates to penetration if violated. In real-world systems, this is infeasible and hence should be minimised. Given this assumption, our proposed regularisation will use the second-order contact derivative and assume that since we are working with low velocities, the second term in Equation 7 will be negligible. As a result, we will use $\mathbf{u}^T (\mathbf{J}_C \dot{\mathbf{q}}) \geq 0$ as the **impenetrability constraint** in our work which will be embedded in our learning objective as explained in Section 4.

4. Physics-Guided Neural Networks for Non-Smooth Dynamics Models

Model-based learning provides an attractive alternative approach to analytically computing Equation 2 to obtain a better model. The standard forward model of a robot, given by Equation 2, can be learned through a data-driven approach. In this manner, a non-linear regression method such as a feedforward neural network (FFNN) learns directly from measured data of an observed trajectory. Predominantly, learning a smooth forward dynamics model is achieved by fitting a function $f_{NN}(\cdot)$, which maps the joint states $(\mathbf{q}, \dot{\mathbf{q}})$ and commanding torques and applying forces $\boldsymbol{\tau}$ to joint accelerations $\ddot{\mathbf{q}}$. For constrained motion in the presence of contacts, this would also include external forces stemming from this interaction. Moreover, we will introduce $\phi_c \in \{0, 1\}$ which is a binary contact activation term that is activated when two bodies are in contact. Mathematically, given a collection of training pairs $\mathcal{D}_{tr} = \{q_i, \dot{q}_i, \tau_i, u_i, \phi_c\}_{i \in 1 \dots \mathcal{D}_{tr}}$, $f_{NN}(\cdot)$ predicts the next state \ddot{q}_i . This is illustrated by Equation 8, where θ are the learnable parameters of the architecture.

$$\ddot{\mathbf{q}} = f_{NN}(\mathbf{q}, \dot{\mathbf{q}}, \boldsymbol{\tau}, \mathbf{u}, \phi_C, \theta) \quad (8)$$

Our choice of neural networks is motivated by the fact that this learning mechanism has shown unparalleled results in learning both forward and inverse dynamics (Chua et al. (2018), Lutter et al. (2019)). In this scenario, the inputs to the NN are the robot's states, action, contact activation and normal, making the input layer equal to $3n+4$, with n being the degrees-of-freedom. The network's predictions are the robot's joint acceleration $\ddot{\mathbf{q}} \in \mathbb{R}^n$.

A standard approach for updating the model described by Equation 8 is to minimise the empirical loss of its predictions on the training set, given the target output, through the mean squared error (MSE). This is a regular supervised learning objective given as follows:

$$\mathcal{L}_{MSE} = \frac{1}{n} \sum_i^n (\hat{\mathbf{q}}_i - \ddot{\mathbf{q}}_i)^2 \quad (9)$$

For our problem, $\hat{\mathbf{q}}_i$ and $\ddot{\mathbf{q}}_i$ represent the predicted and actual accelerations respectively, analytically formulated through a constrained version of Equation 2. However, this loss purely attempts to learn the next state by fitting observed data. There is no guarantee that models generated by minimising Equation 9 will produce results that are consistent with our knowledge of physics. Moreover, such models often fail to generalise, especially when provided with limited observation data. In our particular case, since we are dealing with discontinuous dynamics, making and breaking contact results in a significant challenge. This could potentially lead to high impact dynamics, which would be unsafe especially in the presence of humans.

4.1. Using Physics-based Loss Functions

Instead of relying only on minimising Equation 8, we propose a loss function term that should not cause penetration and produces $\ddot{\mathbf{q}}$ that is normal to the contact force (Lynch and Park (2017)). In simpler terms, the role of this loss is as a physical inconsistency term which penalises physically inconsistent predictions.

Impenetrability Loss: Our proposed loss accounts for Equations 6 and 7, such that $\mathbf{u}^T(\mathbf{J}_C \dot{\mathbf{q}}) = 0$ when two bodies are in contact and $\mathbf{u}^T(\mathbf{J}_C \dot{\mathbf{q}}) > 0$ otherwise. This will result in non-penetration. Furthermore, the learning objective should penalise in cases where $\mathbf{u}^T(\mathbf{J}_C \dot{\mathbf{q}}) < 0$, as this will lead to penetrating solutions. This is analogous to formulating the following loss:

$$\mathcal{L}_{IMP} = \mathbf{u}^T \mathbf{J}_C \ddot{\mathbf{q}} \geq 0 \quad (10)$$

Similar to Equation 7 we again follow the assumption that the velocities will be small and thus $\mathbf{J}_C \dot{\mathbf{q}}$ can be omitted.

4.2. Overall Learning Objective

Our models are trained by combining our proposed physics-guided loss term (Equation 10) with the learning objective of the neural network (Equation 9) using a trade-off weight hyperparameter, λ_{IMP} . Formulating the training objective in this manner stems from the field of multi-task learning (Ruder (2017)), where traditionally multiple tasks are represented by different losses. Our approach leans more towards the science-guided learning method (Karpatne et al. (2017)) as the motivation for combining losses is such that physics knowledge augments the data-driven approach to provide more physically plausible predictions. Hence, our overall learning objective can be framed as follows:

$$\mathcal{L}_{PGNNFDIC} = \mathcal{L}_{MSE} + \lambda_{IMP} \mathcal{L}_{IMP} \quad (11)$$

The empirical loss \mathcal{L}_{MSE} is the general supervised learning objective and the physics-guided loss term \mathcal{L}_{IMP} is essential to penalise predictions that violate the impenetrability constraint. As we use ϕ_c to determine whether the two bodies are in contact, \mathcal{L}_{IMP} is only added when $\phi_c = 1$. Otherwise, we have a system that is governed by the free motion differential equation (2) and hence the overall loss reduces to \mathcal{L}_{MSE} .

Another important factor that helps improve the performance of such regularisation approaches is the choice of λ_{IMP} . In this case, λ_{IMP} is kept constant across all epochs of gradient descent. Inherently, this assumes that \mathcal{L}_{IMP} guides the learning of the neural network towards a generalisable solution, constantly throughout all stages. In practice, Elhamod et al. (2020) showed empirically

that combined losses compete with each other and as a result they should be adaptively tuned. As illustrated in their work, when the loss plays an important role at the early stages where gradient descent tends to approach a local minima, a large value of λ should be set during the initial epochs and decays over time. On the other hand, if the loss is susceptible to favouring the learning of non-generalisable solutions as a result of its high non-convexity, λ should be cold started by initialising to 0 and increasing its value to a constant for later epochs.

5. Experimental Evaluation

To evaluate the efficacy of our proposed physics-penalised regularisation for learning discontinuous dynamics, we performed experiments on a simulated 7 degree-of-freedom robotic manipulator. The experimental evaluation was carried out using an Intel i7-7820X CPU with 3.60GHz, 16 GB memory and NVIDIA GeForce GTX 1080 Ti GPU. The framework was developed using PyTorch ([Paszke et al. \(2019\)](#)).

5.1. Models

For all models, we use three fully connected hidden layers with 21 neurons each and nonlinear rectified linear units (ReLU) activation functions ([Nair and Hinton \(2010\)](#)). The optimal architecture was empirically decided after trying out different depth and width of the network. The inputs to the network were normalised to have zero mean and scaled to unit variance.

FFNN (baseline): As a baseline, we consider the unstructured vanilla feedforward neural network (FFNN) model with a regular supervised learning objective \mathcal{L}_{MSE} . In this instance, no prior knowledge of physics was included. The role of the baseline is to evaluate the prediction quality, i.e. the ability of standard FFNNs to learn discontinuous dynamics.

PGNNFDIC (ours): Our model (Physics-Guided Neural Networks For Dynamics in Contact (PGNNFDIC)) is also an end-to-end FFNN with the addition of an impenetrability constraint (Equation 10) to obtain the combined physics-based loss function (Equation 11). This approach differs from black-box models as it penalises negativity of Equation 10, which is imperative when two bodies are in contact.

5.2. Experimental Setup

5.2.1. ENVIRONMENT

We run experiments using MuJoCo simulator ([Todorov et al. \(2012\)](#)) and we use the simulated fixed-base Franka Emika Panda arm (Figure 1). The end effector comprises a cone (for single-point contacts) with height 40mm and base radius of 30mm scaled at $\{0.0014\ 0.0014\ 0.0014\}$ to replace the conventional FE Gripper. To record impact behaviour, we introduce a plane of size $0.6 \times 0.475 \times 0.1$ positioned at $\{0.8, 0.115, 0.28\}$. As we assess the performance of our model with different contact normals, we use the following plane inclination $\{0^\circ, 45^\circ\}$.

5.2.2. DATA COLLECTION

Our novel regularisation method aims at circumventing the discontinuous nature of dynamics models when exposed to environmental contacts. As a result, we collect data from different trajectories

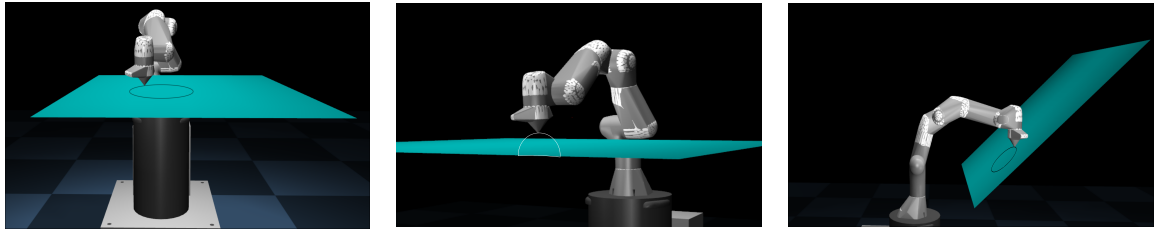


Figure 1: The environment for our experiment comprises the Franka Emika Panda arm following a circular trajectory traversing planes inclined at $\{0^\circ, 45^\circ\}$. Starting from the left, the first image illustrates the horizontal flat plane environment, where the trajectory would exhibit contact for more than 90% of its duration. The second image depicts the manipulator following a vertical circle which would lead to a trajectory that is approximately equally split into free and constrained motion. The third image outlines the manipulator traversing a horizontal circular path along a plane inclined at 45° .

that includes both smooth and non-smooth dynamics. The task was comprised of tracing a circular path parameterised by $[a, r \cos \theta, r \sin \theta] \forall \theta \in [0, 2\pi]$.

The duration of the motion was specified to 100 points along the circular trajectory, discretised at a rate of 100Hz resulting in a total of up to 10k timesteps. The robotic manipulator uses a computed torque controller to follow the circular path and records the data with K_P and K_D set to 180 and 120 respectively. We develop two versions of the task: the first using a flat plane and the second using an inclined plane at 45° . A total of 60 trajectories are generated for each environment with different values of circle radii r and translation in $\{x, y, z\}$. For each trajectory, 90% of the normalised data was used for training and validation (80:20), whereas 10% was used for testing.

5.2.3. LEARNING DISCONTINUOUS DYNAMICS MODELS

In this experiment, we evaluate our proposed *PGNNFDIC* model on the test dataset outlined previously (Section 5.2.2) for its ability to learn discontinuous dynamics models. For evaluation, we use the ADAM optimiser (Kingma and Ba (2014)) with a learning rate of 10^{-3} and a batch size of 16. All the dynamics models are trained with early stopping that leads to termination when the validation loss does not improve for 20 consecutive epochs. Moreover, λ_{IMP} is heuristically tuned to 50 and kept fixed throughout.

We evaluate the system in three scenarios that aim to cover different conditions: (1) flat plane with horizontal circle of $r \in \{0.05, 0.06, 0.065\}$, (2) 45 degree plane with horizontal circle of $r \in \{0.065, 0.07, 0.075, 0.08\}$ and (3) all data which includes (1) and (2) in addition to flat plane with vertical circle of $r \in \{0.06, 0.075\}$. The importance of adding (3) with a vertical circle on the flat plane is to introduce trajectories that also include contact-free dynamics in our trajectories. The results obtained are tabulated in Table 1. Here, we can see that using the model with the impenetrability loss leads to lower MSE when compared to the baseline. Notably, it is evident that our proposed method outperforms the baseline across all scenarios. However, whilst it performs significantly better in the presence of non-smooth dynamics (flat and 45 degree plane), with more

Environment	Model	Average Test MSE
Flat plane	FFNN (baseline)	1.744
	PGNNFDIC (ours)	0.221
45 degree plane	FFNN (baseline)	4.880
	PGNNFDIC (ours)	0.274
All data	FFNN (baseline)	2.658
	PGNNFDIC (ours)	1.406

Table 1: The performance of the system for learning discontinuous dynamics in three scenarios and the mean squared error averaged across different test trajectories. The MSE is a standardised value of the predicted acceleration (rad/s^{-2}). We average our results over three random seeds.

Training Environment / Testing Environment	Model	Average Test MSE
Flat Plane / 45 Degree Plane	FFNN (baseline)	5.633
	PGNNFDIC (ours)	1.318
45 Degree Plane / Flat Plane	FFNN (baseline)	2.497
	PGNNFDIC (ours)	0.529

Table 2: The performance of the system for generalising to a different contact normal and the mean squared error averaged over the test trajectories. The MSE is a standardised value of the predicted acceleration (rad/s^{-2}). The results are averaged over three random seeds.

smooth dynamics introduced in the scenario of all data, our proposed system still suffers from this sharp transition.

5.2.4. GENERALISATION ABILITY

In this experiment, we evaluate how using our novel loss formulation helps learned discontinuous dynamics models to generalise to unseen contact normals. The evaluation is carried out using the test dataset outlined formerly (Section 5.2.2) with the same model parameters aformentioned. To illustrate the generalisation capability of our method, we train and validate the models on the trajectories recorded from a flat plane environment, and test on an inclined plane at 45 degrees. Conversely, we train and validate the models on the trajectories recorded from an inclined plane at 45 degrees, and test on an flat plane. In Table 2 we report the results for our experiments. Once again, we can see that using the model with the impenetrability loss leads to lower MSE when compared to the baseline. Particularly, it is evident that our proposed method outperforms the baseline across both contexts. Similar to the results obtained in Section 5.2.3, we believe that our model’s strength lies in its ability to learn dynamics when in contact and as a result training the model in a scenario with less contact data would not hinder its performance.

6. Conclusion

In this work, we demonstrate how to leverage physics-based regularisation for learning discontinuous dynamics models in an end-to-end model. Our approach adopts a novel impenetrability constraint in the loss function that penalises predictions with high penetration and not perpendicular to the contact normal. As we move closer towards systems that would be applicable to real-world environments, incorporating this knowledge can provide a seemingly simple yet elegant method to generate safer predicted accelerations and a more interpretable dynamics model. Empirically we show how this approach outperforms using feedforward neural networks with regular supervised learning objectives. Using a simulated environment, we evaluate our approach on different trajectories recorded from a seven degree-of-freedom robotic manipulator. Our experimental evaluation offers compelling evidence that there are benefits to modifying the optimisation landscape towards physically-guided results. As illustrated by [Parmar et al. \(2020\)](#), contact-induced discontinuity provides a non-trivial challenge for deep learning and our approach is an attempt to address this issue related to the non-uniqueness state at impact. In future endeavours, we will extend this work for multi-body contact and embed the dynamics model for robotic planning and control. In addition, we aim to investigate further how adaptively tuning the trade-off weight hyperparameter in the physics-based loss would affect the overall performance.

Acknowledgments

This work has received funding from the EPSRC UK RAI Hub National Centre for Nuclear Robotics (NCNR) under agreement EPR02572X/1. The authors are thankful to Jacopo de Berardinis for all his support and feedback about this work and Joshua Smith for his feedback on the manuscript.

References

- A. Ajay, Jiajun Wu, N. Fazeli, M. Bauzá, L. Kaelbling, J. Tenenbaum, and A. Rodríguez. Augmenting physical simulators with stochastic neural networks: Case study of planar pushing and bouncing. *2018 IEEE/RSJ International Conference on Intelligent Robots and Systems (IROS)*, pages 3066–3073, 2018.
- M. Asenov, M. Burke, D. Angelov, T. Davchev, K. Subr, and S. Ramamoorthy. Vid2param: Modeling of dynamics parameters from video. *IEEE Robotics and Automation Letters*, 5(2):414–421, 2020. doi: 10.1109/LRA.2019.2959476.
- M. Azad, V. Ortenzi, H. Lin, E. Rueckert, and M. Mistry. Model estimation and control of compliant contact normal force. In *2016 IEEE-RAS 16th International Conference on Humanoid Robots (Humanoids)*, pages 442–447, 2016. doi: 10.1109/HUMANOIDS.2016.7803313.
- R. Calandra, S. Ivaldi, M. Deisenroth, Elmar A. Rückert, and Jan Peters. Learning inverse dynamics models with contacts. *2015 IEEE International Conference on Robotics and Automation (ICRA)*, pages 3186–3191, 2015.
- K. Chua, R. Calandra, R. McAllister, and S. Levine. Deep reinforcement learning in a handful of trials using probabilistic dynamics models. *Proceedings of the 32nd International Conference on Neural Information Processing Systems*, pages 4759 – 4770, 2018.

- M. Deisenroth, C. Rasmussen, and D. Fox. Learning to control a low-cost manipulator using data-efficient reinforcement learning. In *Robotics: Science and Systems*, 2011.
- M. Elhamod, J. Bu, C. Singh, M. Redell, A. Ghosh, V. Podolskiy, W. Lee, and A. Karpatne. Cophy-pgnn: Learning physics-guided neural networks with competing loss functions for solving eigenvalue problems, 2020.
- N. Fazeli, R. Kolbert, R. Tedrake, and A. Rodriguez. Parameter and contact force estimation of planar rigid-bodies undergoing frictional contact. *The International Journal of Robotics Research*, 36:027836491769874, 04 2017. doi: 10.1177/0278364917698749.
- N. Fazeli, A. Ajay, and A. Rodriguez. Long-horizon prediction and uncertainty propagation with residual point contact learners. In *2020 IEEE International Conference on Robotics and Automation (ICRA)*, pages 7898–7904, 2020. doi: 10.1109/ICRA40945.2020.9196511.
- J. G. Garcia, A. Robertsson, J. Gomez Ortega, and R. Johansson. Generalized contact force estimator for a robot manipulator. In *Proceedings 2006 IEEE International Conference on Robotics and Automation, 2006. ICRA 2006.*, pages 4019–4024, 2006. doi: 10.1109/ROBOT.2006.1642319.
- M. Halm and M. Posa. Modeling and analysis of non-unique behaviors in multiple frictional impacts. *ArXiv*, abs/1902.01462, 2019.
- K. Hitzler, F. Meier, S. Schaal, and T. Asfour. Learning and adaptation of inverse dynamics models: A comparison. In *2019 IEEE-RAS 19th International Conference on Humanoid Robots (Humanoids)*, pages 491–498, 2019. doi: 10.1109/Humanoids43949.2019.9035048.
- Y. Jiang and C. Liu. Data-augmented contact model for rigid body simulation. *ArXiv*, abs/1803.04019, 2018.
- A. Karpatne, G. Atluri, J. Faghmous, M. Steinbach, A. Banerjee, A. Ganguly, S. Shekhar, N. Samatova, and V. Kumar. Theory-guided data science: A new paradigm for scientific discovery. *IEEE Transactions on Knowledge and Data Engineering*, PP, 01 2017. doi: 10.1109/TKDE.2017.2720168.
- D. Kingma and J. Ba. Adam: A method for stochastic optimization. *International Conference on Learning Representations*, 12 2014.
- A. Kloss, S. Schaal, and J. Bohg. Combining learned and analytical models for predicting action effects. *The International Journal of Robotics Research*, 10 2017. doi: 10.1177/0278364920954896.
- M. Lutter, C. Ritter, and J. Peters. Deep lagrangian networks: Using physics as model prior for deep learning. In *7th International Conference on Learning Representations (ICLR)*. ICLR, May 2019. URL <https://openreview.net/pdf?id=BklHpjCqKm>.
- K.M. Lynch and F.C. Park. *Modern Robotics: Mechanics, Planning, and Control*. Cambridge University Press, 2017. ISBN 9781316609842. URL <https://books.google.co.uk/books?id=8uS3AQAAQAAJ>.

- N. Marturi, A. Rastegarpanah, V. Rajasekaran, V. Ortenzi, Y. Bekiroglu, J. Kuo, and R. Stolkin. Towards advanced robotic manipulations for nuclear decommissioning. In Hüseyin Canbolat, editor, *Robots Operating in Hazardous Environments*, chapter 3. IntechOpen, Rijeka, 2017. doi: 10.5772/intechopen.69739. URL <https://doi.org/10.5772/intechopen.69739>.
- V. Nair and G. Hinton. Rectified linear units improve restricted boltzmann machines. pages 807–814, 2010. URL <http://dblp.uni-trier.de/db/conf/icml/icml2010.html#NairH10>.
- D. Nguyen-Tuong and J. Peters. Model learning for robot control: A survey. *Cognitive processing*, 12:319–40, 04 2011. doi: 10.1007/s10339-011-0404-1.
- M. Parmar, M. Halm, and M. Posa. Fundamental challenges in deep learning for stiff contact dynamics. 2020. URL <https://dair.seas.upenn.edu/wp-content/uploads/Parmar2020.pdf>.
- A. Paszke, S. Gross, F. Massa, A. Lerer, J. Bradbury, G. Chanan, T. Killeen, Z. Lin, N. Gimelshein, L. Antiga, A. Desmaison, A. Kopf, E. Yang, Z. DeVito, M. Raison, A. Tejani, S. Chilamkurthy, B. Steiner, L. Fang, J. Bai, and S. Chintala. Pytorch: An imperative style, high-performance deep learning library. In *Advances in Neural Information Processing Systems 32*, pages 8024–8035. Curran Associates, Inc., 2019.
- S. Pfrommer, M. Halm, and M. Posa. Contactnets: Learning discontinuous contact dynamics with smooth, implicit representations, 2020.
- M. Raissi, Paris P. Perdikaris, and George Karniadakis. Physics informed deep learning (part i): Data-driven solutions of nonlinear partial differential equations. 11 2017.
- S. Ruder. An overview of multi-task learning in deep neural networks, 2017.
- L. Sentis. *Compliant Control of Whole-body Multi-contact Behaviors in Humanoid Robots*, pages 29–66. Springer London, London, 2010. ISBN 978-1-84996-220-9. doi: 10.1007/978-1-84996-220-9_2. URL https://doi.org/10.1007/978-1-84996-220-9_2.
- B. Siciliano and O. Khatib. *Springer Handbook of Robotics*. Springer Handbooks. Springer International Publishing, 2016. ISBN 9783319325521. URL <https://books.google.co.uk/books?id=RTvADAAAQBAJ>.
- E. Todorov, T. Erez, and Y. Tassa. Mujoco: A physics engine for model-based control. In *2012 IEEE/RSJ International Conference on Intelligent Robots and Systems*, pages 5026–5033, 2012. doi: 10.1109/IROS.2012.6386109.
- J. Willard, X. Jia, S. Xu, M. Steinbach, and V. Kumar. Integrating physics-based modeling with machine learning: A survey, 2020.